Adaptive Window Width Control for Cyclic Shifted Pilot Aided Channel Estimation Suitable for SC-ANC Bi-Directional Relay Using Joint Tx/Rx MMSE-FDE

Hiroyuki MIYAZAKI† Tatsunori OBARA† and Fumiyuki ADACHI‡
Dept. of Communications Engineering, Graduate School of Engineering, Tohoku University
6-6-05 Aza-Aoba, Aramaki, Aoba-ku, Sendai, 980-8579 Japan
†{miyazaki, obara}@mobile.ecei.tohoku.ac.jp, ‡adachi@ecei.tohoku.ac.jp

***Abstract*—In analog network coded (ANC) relay with conventional channel estimation, the feedback of the estimated channel state information (CSI) is required, and hence, the bandwidth efficiency decreases. A cyclic-shifted pilot aided channel estimation (CSPACE) is used to simultaneously estimate two equivalent channels which are required for joint transmit/receive frequency-domain equalization (FDE) and own transmitted signal removal and hence, it requires no CSI feedback. In CSPACE, the delay time-domain windowing is used to separate two equivalent channels and suppress the impact of noise. However, in single-carrier (SC) ANC multi-antenna bi-directional relay (SC-ANC-MBDR) with the joint transmit/receive FDE, the equivalent channel is a concatenation of the propagation channel and the transmit FDE, and hence, its impulse response spreads over the entire delay time-domain. Therefore, the optimal delay time-domain window varies according to changing instantaneous received signal-to-noise power ratio (SNR), and as a consequence, the channel estimation accuracy degrades if the window width for the delay time-domain windowing is not adapted to the instantaneous received SNR. In this paper, we propose an adaptive window width control (AWWC) for CSPACE. The proposed AWWC adaptively changes the window size so as to minimize the mean square error (MSE) between the channel estimate and the actual channel. It is confirmed by the computer simulation that CSPACE using our proposed AWWC can always achieve BER performance superior to when using fixed window width.**

Keywords-component; Analog network coding, single-carrier transmission, channel estimation

I. INTRODUCTION

In broadband data transmissions, the received signal suffers from propagation path loss, shadowing loss and frequency selective fading [1]. Cooperative relay is a promising technique to overcome the impact of the propagation path loss and the shadowing loss [2]. There are two relay protocols; amplify-and-forward (AF) relay and decode-and-forward (DF) relay [2]. The cooperative AF relay can improve the cell edge throughput performance while reducing complexity and signal processing delay compared to the cooperative DF relay. However, the cooperative relay requires four time-slots for bi-directional communications while conventional direct communications requires two time-slots. Therefore, the cooperative relay communications reduces the achievable maximum throughput to half of the direct communications.

An application of analog network coding (ANC) [3-5] is an effective way to improve the throughput performance for bi-directional relay (BDR). ANC uses two time-slots for BDR, and hence, it can achieve the same maximum throughput as the direct communications while mitigating the impact of the propagation path loss and the shadowing loss. To further improve the throughput performance, ANC multi-antenna BDR (ANC-MBDR) has been studied in [6,7]. The spatial diversity gain can be obtained by employing transmit diversity at relay station (RS). Recently, we proposed a joint transmit/receive minimum mean square error (MMSE) based frequency-domain equalization (FDE) for single-carrier (SC) ANC-MBDR (SC-ANC-MBDR) [8]. We showed that the proposed joint transmit/receive MMSE-FDE provides the bit error rate (BER) performance superior to the receive FDE [8]. However, in [8], the perfect channel estimation was assumed.

Channel estimation (CE) for ANC-BDR has been studied in [9,10]. The conventional CE proposed in [9] requires the feedback of the estimated channel state information (CSI), and hence, the bandwidth efficiency reduces. On the other hand, the cyclic-shifted pilot aided channel estimation (CSPACE) proposed in [10] simultaneously estimates two equivalent channels which are required for the joint transmit/receive FDE and own transmitted signal removal. Therefore, CSPACE requires no CSI feedback. In CSPACE, the delay time-domain windowing [11] is used to separate two equivalent channels and suppress the impact of the noise. However, using joint transmit/receive MMSE-FDE, since the equivalent channel is a concatenation of the propagation channel and the transmit FDE, its impulse response spreads over the entire delay time-domain. Thus, the optimal delay time-domain window varies according to the changing instantaneous received signal-to-noise power ratio (SNR). As a consequence, the channel estimation accuracy degrades if the delay time-domain window is not adapted to the changing instantaneous received SNR.

In this paper, we propose an adaptive window width control (AWWC) for CSPACE suitable for SC-ANC-MBDR using the joint transmit/receive MMSE-FDE. The proposed AWWC adaptively changes the window width so as to minimize the mean square error (MSE) between the channel estimate and the actual channel. It is shown by computer simulations that CSPACE with our proposed AWWC can achieve better BER and throughput performances than CSPACE with fixed window width and the conventional CE [9].

The remainder of this paper is organized as follows. Section II describes the system model and signal representation. CSPACE is presented in Sect. III and AWWC is proposed in Sect. IV. Section V discusses the computer simulation results, and Sect. VI offers conclusions.

II. Multi-Antenna ANC Bi-Directional Relay Communications

A. System model

In this paper, we consider SC-ANC-MBDR using the joint transmit/receive MMSE-FDE [8]. The system model considered in this paper is illustrated in Fig. 1. The relay station (RS) which is equipped with J antennas is located between the base station (BS) and the mobile terminal (MT). We assume BS and MT equip with single antenna, respectively.

ANC requires two time-slots for bi-directional relay communications. In the first time-slot, BS and MT simultaneously transmit their signals to RS. Then RS carries out the transmit FDE to the receive signal. In the second time-slot, RS amplifies the equalized signal and broadcasts it to BS and MT. At BS and MT receivers, the receive FDE is carried out after own transmitted signal removal.

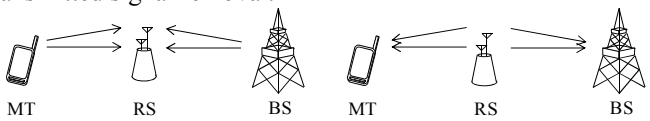

(a) First time-slot (b) Second time-slot

Fig. 1 ANC protocol.

B. Signal representation

In this paper, symbol-spaced discrete time signal representation is used.

(a) First time-slot

The data symbol blocks of N_c symbols are generated at BS and MT, respectively. After insertion of N_g sample cyclic prefix (CP) into the beginning of each block, BS and MT simultaneously transmit their symbol blocks to RS in the first time-slot. At RS, after CP removal, the receive signal is transformed into the frequency-domain signal by N_c-point fast Fourier transform (FFT). The frequency-domain receive signal, $\{Y_R(j,k) : k=0,\ldots,N_c-1\}$, at jth RS antenna can be expressed as

$$\begin{aligned} Y_R(j,k) &= \sqrt{2P_B}\,H_{B-R}(j,k)X_B(k) \\ &\quad + \sqrt{2P_M}\,H_{M-R}(j,k)X_M(k) + N_R(j,k) \end{aligned}. \quad (1)$$

In (1), P_B and P_M are the transmit power of BS and MT, respectively. $H_{B\text{-}R}(j,k)$ and $H_{M\text{-}R}(j,k)$ denote the channel transfer functions between BS and jth RS antenna and between MT and jth RS antenna, respectively. $N_R(j,k)$ is the independent zero-mean complex-valued additive white Gaussian noise (AWGN) having variance $2N_0/T_s$ with N_0 and T_s being the single-sided power spectrum density of the AWGN and the symbol duration. $X_B(k)$ and $X_M(k)$ are the kth frequency components of the transmitted signal of BS and MT, respectively. RS performs FDE to the frequency-domain received signal. The frequency-domain signal, $\{\hat{Y}_R(j,k) : k=0,\ldots,N_c-1\}$, after FDE at jth RS antenna is given as

$$\hat{Y}_R(j,k) = G(j)Y_R(j,k)V(j,k), \quad (2)$$

where $V(j,k)$ denotes the transmit FDE weight at jth RS antenna and $G(j)$ is the amplifying factor at jth RS antenna, respectively. The amplifying factor $G(j)$ is set so as to keep the average transmit power of RS constant as

$$G(j) = \sqrt{\frac{P_R}{\frac{P_B}{N_c}\sum_{k=0}^{N_c-1}|H_{B-R}(j,k)|^2 + \frac{P_M}{N_c}\sum_{k=0}^{N_c-1}|H_{M-R}(j,k)|^2 + N}}, \quad (3)$$

where P_R is the transmit power of RS and $N=N_0/T_s$ is the noise power.

(b) Second time-slot

The frequency-domain signal after FDE is transformed back to the time-domain signal by N_c-point inverse FFT (IFFT). After CP insertion, RS broadcasts it to BS and MT in the second time-slot. After CP removal, the received signals at BS and MT are transformed into the frequency-domain signals by N_c-point FFT. The frequency-domain received signals, $\{Y_B(k) : k=0,\ldots,N_c-1\}$ and $\{Y_M(k) : k=0,\ldots,N_c-1\}$, at BS and MT can be respectively expressed as

$$\begin{cases} Y_B(k) = H_{M-R-B}(k)X_M(k) + H_{B-R-B}(k)X_B(k) + \tilde{N}_B(k) \\ Y_M(k) = H_{B-R-M}(k)X_B(k) + H_{M-R-M}(k)X_M(k) + \tilde{N}_M(k) \end{cases}, \quad (4)$$

where $H_{B\text{-}R\text{-}B}(k)$ and $H_{M\text{-}R\text{-}M}(k)$ denote the equivalent channel gains between BS and BS via RS and between MT and MT via RS, respectively. They are given as

$$\begin{cases} H_{B-R-B}(k) = \sqrt{2P_B}\sum_{j=0}^{J-1} H_{B-R}(j,k)H_{B-R}(j,k)V(j,k) \\ H_{M-R-M}(k) = \sqrt{2P_M}\sum_{j=0}^{J-1} H_{M-R}(j,k)H_{M-R}(j,k)V(j,k) \end{cases}. \quad (5)$$

$H_{M\text{-}R\text{-}B}(k)$ and $H_{B\text{-}R\text{-}M}(k)$ are the equivalent channel gains between MT and BS and between BS and MT, respectively. They are given as

$$\begin{cases} H_{M-R-B}(k) = \sqrt{2P_M}\sum_{j=0}^{J-1} H_{B-R}(j,k)H_{M-R}(j,k)V(j,k) \\ H_{B-R-M}(k) = \sqrt{2P_B}\sum_{j=0}^{J-1} H_{M-R}(j,k)H_{B-R}(j,k)V(j,k) \end{cases}. \quad (6)$$

$\tilde{N}_B(k)$ and $\tilde{N}_M(k)$ are the noises at BS and MT including the noise which is amplified and forward by RS, respectively. The own transmitted signal is removed from the received signal as

$$\begin{cases} \tilde{Y}_B(k) = Y_B(k) - H_{B-R-B}(k)X_B(k) \\ \tilde{Y}_M(k) = Y_M(k) - H_{M-R-M}(k)X_M(k) \end{cases}. \quad (7)$$

After own transmitted signal removal, the receive FDE is carried out. The received signals after the receive FDE $\{\hat{Y}_B(k) : k=0,\ldots,N_c-1\}$ and $\{\hat{Y}_M(k) : k=0,\ldots,N_c-1\}$, at BS and MT are given as

$$\begin{cases} \hat{Y}_B(k) = \tilde{Y}_B(k)W_B(k) \\ \hat{Y}_M(k) = \tilde{Y}_M(k)W_M(k) \end{cases}, \quad (8)$$

where $W_B(k)$ and $W_M(k)$ are the receive FDE weights at BS and MT, respectively. The receive signals after FDE are transformed back to the time-domain signal by N_c-point IFFT, and the data demodulation is carried out.

C. Transmit/receive FDE weights

The joint transmit/receive FDE weights at RS, BS and MT are determined so as to minimize the end-to-end MSE of uplink and downlink [8]. The transmit FDE weight at RS is given as [8]

$$V(j,k)=\frac{G(j)\widetilde{H}^{*}_{M-R}(j,k)\widetilde{H}^{*}_{B-R}(j,k)}{\sqrt{A(k)}} \cdot\sqrt{\max\left[\frac{\sqrt{(2\sigma_R^2A(k))/\lambda}-2\sigma_R^2}{A(k)+2\sigma_R^2(B(k)/A(k))},\ 0\right]}, \quad (9)$$

where

$$\begin{cases}A(k)=\sum_{j=0}^{J-1}\left|G(j)\widetilde{H}_{M-R}(j,k)\widetilde{H}_{B-R}(j,k)\right|^2\\ B(k)=\sum_{j=0}^{J-1}\left|G(j)\widetilde{H}_{M-R}(j,k)\widetilde{H}_{B-R}(j,k)\right|^2\left|G(j)\widetilde{H}_{M-R}(j,k)\right|^2\end{cases}, \quad (10)$$

and

$$\begin{cases}\widetilde{H}_{M-R}(j,k)=\sqrt{2P_M}H_{M-R}(j,k)\\ \widetilde{H}_{B-R}(j,k)=\sqrt{2P_B}H_{B-R}(j,k)\end{cases}. \quad (11)$$

σ_R^2 denotes the noise power at RS. λ is a constant value and set so as to keep the transmit power of RS constant. The receive FDE weights at BS and MT are given as

$$\begin{cases}W_B(k)=\dfrac{H^{*}_{M-R-B}(k)}{\left|H_{M-R-B}(k)\right|^2+2\sigma_B^2}\\ W_M(k)=\dfrac{H^{*}_{B-R-M}(k)}{\left|H_{B-R-M}(k)\right|^2+2\sigma_M^2}\end{cases}, \quad (12)$$

where σ_B^2 and σ_M^2 are the received noise powers at BS and MT, respectively.

From (9), RS need to estimate the channels between BS and *j*th RS antenna and between MT and *j*th RS antenna, respectively. On the other hand, from (7) and (12), MT (BS) need only to estimate the equivalent channels between MT and MT via RS and between BS and MT (BS and BS via RS and between MT and BS), respectively.

III. Channel Estimation for SC-ANC-MBDR

We assume the channel estimation using cyclic-shifted time-domain multiplexed pilots [11]. The transmission frame is shown in Fig. 2. The pilot frame is inserted per N_B data symbol blocks. Pilot stage consists of 2 time-slots. In the first time-slot, BS and MT, which has the cyclic shifted versions of the same pilot, simultaneously transmit their pilots to RS. RS estimates the channel gains between BS and RS and between MT and RS, and the noise power, respectively for the computing the transmit FDE weight given as (9). Then, RS multiplies the obtained transmit FDE weights to the frequency-domain received pilots and broadcasts it to BS and MT in the second time-slot. BS (MT) estimates the equivalent channel gains between BS and BS via RS and between MT and BS (between MT and MT via RS and between BS and MT), and the noise power, respectively.

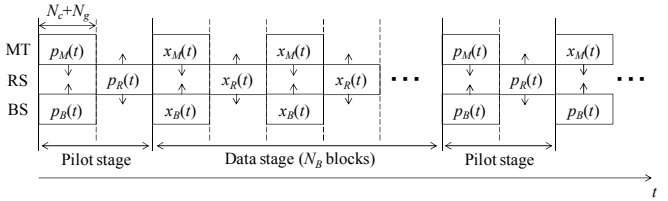

Fig. 2 Transmit frame structure.

A. Channel estimation at RS

The transmit pilot block of N_c samples at BS and MT are denoted as $\{p_B(t) : t=0,\ldots,N_c-1\}$ and $\{p_M(t) : t=0,\ldots,N_c-1\}$, respectively. The transmit pilot at BS is cyclic shifted by θ samples relative to the pilot signal at MT given as $p_B(t)=p_M((t-\theta) \bmod N_c)$. After CP insertion, BS and MT simultaneously transmit their pilots to RS in the first time-slot. After CP removal, the received pilot signal is transformed into the frequency-domain signal. The frequency-domain received pilot, $\{R_R(j,k) : k=0,\ldots,N_c-1\}$, at *j*th RS antenna can be expressed as

$$R_R(j,k)=\left\{\begin{matrix}\widetilde{H}_{M-R}(j,k)\\ +\widetilde{H}_{B-R}(j,k)\exp(-j2\pi k\theta/N_c)\end{matrix}\right\}P_M(k)+N_R(j,k). \quad (13)$$

RS removes the pilot by the reverse modulation as

$$\overline{H}_R(k)=R_R(j,k)\cdot P_M^{*}(k)/\left|P_M(k)\right|^2. \quad (14)$$

The total channel impulse response $\overline{h}_R(j,\tau)$ is obtained by applying N_c-point IFFT to the frequency-domain pilot signal, $\overline{H}_R(k)$, after the inverse modulation. The total channel impulse response $\overline{h}_R(j,\tau)$ can be expressed as

$$\overline{h}_R(j,\tau)=\widetilde{h}_{M-R}(j,\tau)+\widetilde{h}_{B-R}(j,(\tau-\theta) \bmod N_c)+\widetilde{n}_R(j,\tau), \quad (15)$$

where $\widetilde{h}_{M-R}(j,\tau)$ and $\widetilde{h}_{B-R}(j,\tau)$ are the channel impulse responses of the links between MT and *j*th RS antenna and between BS and *j*th RS antenna, respectively. $\widetilde{n}_R(j,\tau)$ denotes the noise component. A delay time-domain windowing is used to separate two channel impulse response estimates as

$$\widetilde{h}_{M-R}(j,\tau)=\begin{cases}\overline{h}_R(j,\tau) & \tau=0,\ldots,N_g-1\\ 0 & \text{otherwise}\end{cases}, \quad (16)$$

and

$$\widetilde{h}_{B-R}(j,\tau)=\begin{cases}\overline{h}_R(j,\tau+\theta) & \tau=0,\ldots,N_g-1\\ 0 & \text{otherwise}\end{cases}. \quad (17)$$

Finally, the channel estimates, $\widetilde{H}_{B-R}(j,k)$ and $\widetilde{H}_{M-R}(j,k)$, of the links between BS and *j*th RS antenna and between MT and *j*th RS antenna are obtained by applying N_c-point FFT to the channel impulse response estimates $\widetilde{h}_{M-R}(j,\tau)$ and $\widetilde{h}_{B-R}(j,\tau)$, respectively. The noise power at RS σ_R^2 is estimated as

$$\sigma_R^2=\frac{1}{2}\frac{1}{N_c-2N_g}\frac{1}{J}\sum_{j=0}^{J-1}\left\{\sum_{\tau=N_g}^{\theta-1}\left|\overline{h}_R(j,\tau)\right|^2+\sum_{\tau=\theta+N_g}^{N_c-1}\left|\overline{h}_R(j,\tau)\right|^2\right\}. \quad (18)$$

After the channel and the noise power estimation, RS computes the transmit FDE weights given as (9). Then RS multiplies the obtained transmit FDE weights to the frequency-domain received pilot signal as

$$P_R(j,k)=G(j)V(j,k)R_R(j,k). \quad (19)$$

The pilot signal multiplied by the transmit FDE weight is transformed back to the time-domain signal by N_c-point IFFT. After CP insertion, RS broadcasts it to BS and MT in the second time-slot.

B. Channel estimation at MT (BS)

BS and MT estimates the equivalent channel gains in the same way. Therefore, the channel estimation at MT is only introduced in this subsection.

After CP removal, the received pilot at MT is transformed into the frequency-domain signal by N_c-point FFT. The frequency-domain received pilot, $\{R_M(k) : k=0,\ldots,N_c-1\}$, at MT can be expressed as

$$R_M(k)=\left.\begin{Bmatrix}H_{M-R-M}(k)\\ +H_{B-R-M}(k)\exp(-j2\pi k\theta/N_c)\end{Bmatrix}\right\}P_M(k)+\tilde{N}_M(k). \quad (20)$$

The pilot is removed by the reverse modulation as

$$\overline{H}_M(k)=R_M(j,k)\cdot P_M^*(k)/|P_M(k)|^2 . \quad (21)$$

The total channel impulse response $\overline{h}_M(\tau)$ is obtained by applying N_c-point IFFT to the signal after the inverse modulation. The total channel impulse response $\overline{h}_M(\tau)$ are given as

$$\overline{h}_M(\tau)=\widetilde{h}_{M-R-M}(\tau)+\widetilde{h}_{B-R-M}((\tau-\theta)\bmod N_c)+\widetilde{n}_M(\tau), \quad (22)$$

where $\widetilde{h}_{M-R-M}(\tau)$ and $\widetilde{h}_{B-R-M}(\tau)$ are the impulse responses of the equivalent channel between MT and MT via RS and between BS and MT, respectively. Therefore, the equivalent channels can be estimated by applying delay time-domain windowing. The impulse response estimates, $\{\widetilde{h}_{M-R-M}(\tau) : \tau=-N_c/2,\ldots,N_c/2\}$ and $\{\widetilde{h}_{B-R-M}(\tau) : \tau=-N_c/2,\ldots,N_c/2\}$, of the equivalent channels are given as

$$\begin{cases}\widetilde{h}_{M-R-M}(\tau)=\overline{h}_M((\tau)\bmod N_c)\omega_{M-R-M}(\tau)\\ \widetilde{h}_{B-R-M}(\tau)=\overline{h}_M((\tau+\theta)\bmod N_c)\omega_{B-R-M}(\tau)\end{cases}, \quad (23)$$

where $\{\omega_{M-R-M}(\tau) : \tau=-N_c/2,\ldots,N_c/2\}$ and $\{\omega_{M-R-M}(\tau) : \tau=-N_c/2,\ldots,N_c/2\}$ are the delay time-domain windows. They are given as

$$\omega_{M-R-M}(\tau)=\begin{cases}1 & w_{M-R-M,1}\le\tau\le w_{M-R-M,2}\\ 0 & \text{otherwise}\end{cases}$$
$$\omega_{B-R-M}(\tau)=\begin{cases}1 & w_{B-R-M,1}\le\tau\le w_{B-R-M,2}\\ 0 & \text{otherwise}\end{cases}, \quad (24)$$

where $w_{M\text{-}R\text{-}M,1}$, $w_{M\text{-}R\text{-}M,2}$, $w_{B\text{-}R\text{-}M,1}$ and $w_{B\text{-}R\text{-}M,2}$ are the window widths. However, since the equivalent channel gains are the concatenations of the propagation channel and the transmit FDE, its impulse response spreads over the entire delay time-domain shown in Fig. 3. Thus, the optimal delay time-domain window varies according to the changing instantaneous received SNR. As a consequence, the channel estimation accuracy degrades if the delay time-domain window is not adapted to the changing instantaneous received SNR. In next section, we propose the delay time-domain windowing with AWWC.

IV. Adaptive Window Width Control

A. Consideration for the optimal window width

The optimal window widths $w_{M-R-M,1}^{opt}$, $w_{M-R-M,2}^{opt}$, $w_{B-R-M,1}^{opt}$ and $w_{B-R-M,2}^{opt}$ are determined so as to minimize the MSEs between the channel impulse response estimates and the actual channel impulse responses as

$$\begin{aligned}&\{w_{M-R-M,1}^{opt},w_{M-R-M,2}^{opt}\}\\ &=\arg\min\sum_{\tau=-N_c/2}^{N_c/2}E\left[\left|\widetilde{h}_{M-R-M}(\tau)-h_{M-R-M}(\tau)\right|^2\right]\\ &\{w_{B-R-M,1}^{opt},w_{B-R-M,2}^{opt}\}\\ &=\arg\min\sum_{\tau=-N_c/2}^{N_c/2}E\left[\left|\widetilde{h}_{B-R-M}(\tau)-h_{B-R-M}(\tau)\right|^2\right]\end{aligned} . \quad (25)$$

(25) can be rewritten as

$$\begin{aligned}&\{w_{M-R-M,1}^{opt},w_{M-R-M,2}^{opt}\}\\ &=\arg\min\left\{\sum_{\tau=w_{M-R-M,1}^{opt}}^{w_{M-R-M,2}^{opt}}2\sigma_M^2+\sum_{\tau=-N_c/2}^{w_{M-R-M,1}^{opt}}|h_{M-R-M}(\tau)|^2+\sum_{\tau=w_{M-R-M,2}^{opt}}^{N_c/2}|h_{M-R-M}(\tau)|^2\right\}\\ &\{w_{B-R-M,1}^{opt},w_{B-R-M,2}^{opt}\}\\ &=\arg\min\left\{\sum_{\tau=w_{B-R-M,1}^{opt}}^{w_{B-R-M,2}^{opt}}2\sigma_M^2+\sum_{\tau=-N_c/2}^{w_{B-R-M,1}^{opt}}|h_{B-R-M}(\tau)|^2+\sum_{\tau=w_{B-R-M,2}^{opt}}^{N_c/2}|h_{B-R-M}(\tau)|^2\right\}\end{aligned} . \quad (26)$$

The first term is the noise power in the delay time-domain window. The second and the third terms are the impulse response powers outside the delay time-domain window. Therefore, the optimal window width can be calculated by estimating the noise power and the channel impulse response power.

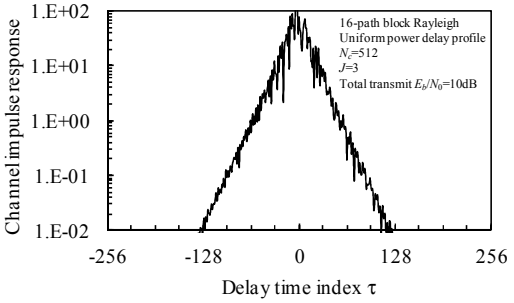

Fig. 3 The impulse response of the equivalent channel ($h_{M\text{-}R\text{-}M}(\tau)$).

B. Adaptive window width control

The flow chart of the proposed delay time-domain windowing with AWWC is shown in Fig. 4. The proposed scheme consists of 4 parts; delay time-domain windowing, noise power estimation, impulse response power estimation and window width updating. The window widths are optimized by iterating the above processes.

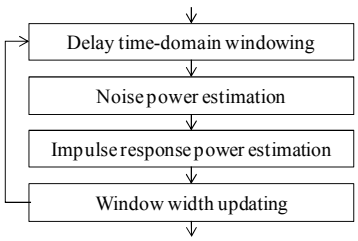

Fig. 4 Flow chart of adaptive window width control.

Below, the ith (i=0,…,I–1) iteration is described. At first, the delay time-domain windowing is performed using (i–1) th window width (When 0th iteration, the fixed window width is used). The impulse response estimates of the equivalent channels, $\widetilde{h}_{M-R-M}^{(i)}(\tau)$ and $\widetilde{h}_{B-R-M}^{(i)}(\tau)$, are given as

$$\begin{cases}\widetilde{h}_{M-R-M}^{(i)}(\tau)=\overline{h}_M((\tau)\bmod N_c)\omega_{M-R-M}^{(i-1)}(\tau)\\ \widetilde{h}_{B-R-M}^{(i)}(\tau)=\overline{h}_M((\tau+\theta)\bmod N_c)\omega_{B-R-M}^{(i-1)}(\tau)\end{cases}. \quad (27)$$

The noise power is estimated as

$$(\sigma_M^{(i)})^2=\frac{1}{2}\frac{1}{N_c-\Omega^{(i)}}\left\{\sum_{\tau=w_{M-R-M,2}^{(i-1)}}^{\theta+w_{M-R-M,1}^{(i-1)}-1}\left|\overline{h}_M(\tau)\right|^2+\sum_{\tau=\theta+w_{B-R-M,2}^{(i-1)}}^{N_c+w_{B-R-M,1}^{(i-1)}-1}\left|\overline{h}_M(\tau)\right|^2\right\} \quad (28)$$

where

$$\Omega^{(i)} = \sum_{\tau=-N_c/2}^{N_c/2} \left\{ \omega_{M-R-M}^{(i-1)}(\tau) + \omega_{B-R-M}^{(i-1)}(\tau) \right\}. \quad (29)$$

Next, the power estimation of impulse response outside the delay time-domain window is performed. As shown in Fig. 3, the impulse response of the equivalent channels can be approximated as exponential function. Based on the above observation, in the proposed scheme, the impulse response outside the window is extrapolated by using exponential function approximation by least square method [12]. The approximated functions, $\{ \hat{h}_{M-R-M}^{(i)}(\tau) : \tau=-N_c/2,\ldots,N_c/2 \}$ and $\{ \hat{h}_{B-R-M}^{(i)}(\tau) : \tau=-N_c/2,\ldots,N_c/2 \}$, by least square method are given as

$$\hat{h}_{M-R-M}^{(i)}(\tau) = \begin{cases} a_{M-R-M,1}^{(i)} \left(b_{M-R-M,1}^{(i)}\right)^{\tau} & 0 \le \tau \le N_c/2 \\ a_{M-R-M,2}^{(i)} \left(b_{M-R-M,2}^{(i)}\right)^{\tau} & -N_c/2 \le \tau < 0 \end{cases}$$
$$\hat{h}_{B-R-M}^{(i)}(\tau) = \begin{cases} a_{B-R-M,1}^{(i)} \left(b_{B-R-M,1}^{(i)}\right)^{\tau} & 0 \le \tau \le N_c/2 \\ a_{B-R-M,2}^{(i)} \left(b_{B-R-M,2}^{(i)}\right)^{\tau} & -N_c/2 \le \tau < 0 \end{cases}, \quad (30)$$

where $a_{M-R-M,1}^{(i)}$, $a_{M-R-M,2}^{(i)}$, $b_{M-R-M,1}^{(i)}$ and $b_{M-R-M,2}^{(i)}$ ($a_{B-R-M,1}^{(i)}$, $a_{B-R-M,2}^{(i)}$, $b_{B-R-M,1}^{(i)}$ and $b_{B-R-M,2}^{(i)}$) are set so as to minimize the sum of square errors between the approximated function $\hat{h}_{M-R-M}^{(i)}(\tau)$ ($\hat{h}_{B-R-M}^{(i)}(\tau)$) and the impulse response estimate $\tilde{h}_{M-R-M}^{(i)}(\tau)$ ($\tilde{h}_{B-R-M}^{(i)}(\tau)$) [12]. Next, the window widths are updated so as to satisfy the simplified optimization problem given as

$$\begin{aligned} &\left\{ w_{M-R-M,1}^{(i)}, w_{M-R-M,2}^{(i)} \right\} \\ &= \arg\min \left\{ \sum_{\tau=w_{M-R-M,1}^{(i-1)}}^{w_{M-R-M,2}^{(i-1)}} 2\left(\sigma_M^{(i)}\right)^2 + \sum_{\tau=-N_c/2}^{w_{M-R-M,1}^{(i-1)}} \left|\hat{h}_{M-R-M}^{(i)}(\tau)\right|^2 + \sum_{\tau=w_{M-R-M,2}^{(i-1)}}^{N_c/2} \left|\hat{h}_{M-R-M}^{(i)}(\tau)\right|^2 \right\} \\ &\left\{ w_{B-R-M,1}^{opt}, w_{B-R-M,2}^{opt} \right\} \\ &= \arg\min \left\{ \sum_{\tau=w_{B-R-M,1}^{(i-1)}}^{w_{B-R-M,2}^{(i-1)}} 2\left(\sigma_M^{(i)}\right)^2 + \sum_{\tau=-N_c/2}^{w_{B-R-M,1}^{(i-1)}} \left|\hat{h}_{B-R-M}^{(i)}(\tau)\right|^2 + \sum_{\tau=w_{B-R-M,2}^{(i-1)}}^{N_c/2} \left|\hat{h}_{B-R-M}^{(i)}(\tau)\right|^2 \right\} \end{aligned}. \quad (31)$$

The solutions of the above optimization problem are given as

$$\begin{cases} w_{M-R-M,1}^{(i)} = \left[\ln \sigma_M^{(i)} - \ln a_{M-R-M,1}^{(i)}\right] / 2 \ln b_{M-R-M,1}^{(i)} \\ w_{M-R-M,2}^{(i)} = \left[\ln \sigma_M^{(i)} - \ln a_{M-R-M,2}^{(i)}\right] / 2 \ln b_{M-R-M,2}^{(i)} \\ w_{B-R-M,1}^{(i)} = \left[\ln \sigma_M^{(i)} - \ln a_{B-R-M,1}^{(i)}\right] / 2 \ln b_{B-R-M,1}^{(i)} \\ w_{B-R-M,2}^{(i)} = \left[\ln \sigma_M^{(i)} - \ln a_{B-R-M,2}^{(i)}\right] / 2 \ln b_{B-R-M,2}^{(i)} \end{cases}. \quad (32)$$

The proposed scheme updates the window widths by using (32). The window widths are optimized by iterating the above processes. After I iterations, the equivalent channel gain estimates, $H_{M-R-M}(k)$ and $H_{B-R-M}(k)$, are obtained by applying N_c-point FFT to the channel impulse response estimates $\tilde{h}_{M-R-M}^{(I-1)}(\tau)$ and $\tilde{h}_{B-R-M}^{(I-1)}(\tau)$.

V. Computer Simulation

We evaluate, by computer simulation, the BER performance and the throughput performance when using CSPACE with the proposed AWWC. We consider QPSK data modulation. FFT block size N_c and CP length N_g are set to N_c=512 and N_g=16, respectively. We assume the total transmit power constraint given as $P_R + P_B + P_M = P_T$, where P_T is the total transmit power. In the computer simulation, the power allocation of P_R=P_T/2 and P_B=P_M= P_T/4 is assumed. We assume a frequency-selective block Rayleigh fading having symbol-spaced L=16-path uniform power delay profile. We consider a quasi-static fading channel (i.e., Doppler frequency $f_D \to 0$) in the computer simulation. We use a Chu-sequence [13] for the pilot signal. The pilot insertion interval N_B is set to N_B=16. The number of iterations I for AWWC is set to I=10.

A. BER performance

Fig. 5 plots the BER performance as a function of the total transmit signal energy per bit-to-AWGN power spectrum density ratio E_b/N_0 ($=0.5 \cdot P_T T_s / N_0 \cdot (1+N_g/N_c) \cdot (1+1/N_B)$) including the pilot insertion loss of 0.26dB. The number of RS antennas is set to J=3. For the comparison, the performance when using fixed window width ($w_{M\text{-}R\text{-}M,1}$=$w_{M\text{-}R\text{-}M,2}$=,…,=$w$) and the performance with perfect CSI are also plotted in Fig. 5. It is seen from Fig. 5 that the optimal window width changes according to the total transmit E_b/N_0. The reason for this is explained as below. In CSPACE, the channel estimation accuracy suffers from the noise and the channel impulse response length. When the total transmit E_b/N_0 is low, the predominant factor to degrade channel estimation accuracy is the additive noise, and hence, the better BER performance can be obtained as the window width is made narrower. On the other hand, the total transmit E_b/N_0 is sufficiently high, the predominant factor to degrade channel estimation accuracy is the channel impulse response length. Therefore, the better BER performance can be obtained as the window width is made wider. It is also seen from Fig. 5 that AWWC always provides the BER performance superior to when using fixed window width. This is because the proposed scheme adaptively determines the window width so as to minimize the channel estimation error. It is also seen from Fig. 5 that CSPACE with AWWC can achieve similar performance to the perfect CSI case. When the required BER is 10^{-4}, E_b/N_0 degradation is about 2dB compared to the perfect CSI case.

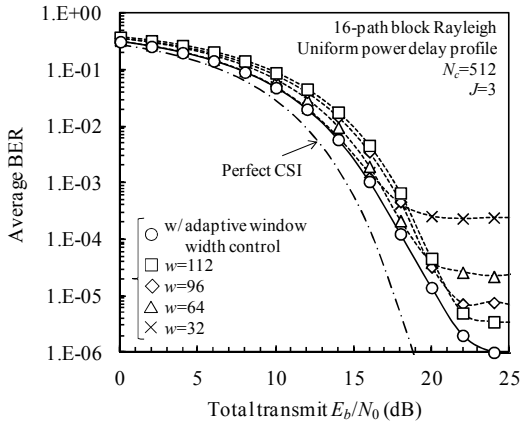

Fig. 5 BER performance.

B. Computational complexity

In this paper, the computational complexity is defined as the number of real multiplications per block. The computational complexity for CSPACE with AWWC is shown in Table 1. The frequency-domain channel estimation (FDCE) re-

quires N_c-point FFT and IFFT, and hence, the computational complexity is proportional to $N_c \log_2 N_c$. On the other hand, AWWC is performed on the delay time-domain only, and hence, the computational complexity is proportional to $I \times N_c$. When N_c=512 and I=10, the computational complexity of AWWC is less than 46120 while that of the frequency-domain channel estimation is 47104. As a consequence, the computational complexity of AWWC is almost same as that of FDCE.

C. Throughput performance

We evaluate the throughput performance when using CSPACE with AWWC and the conventional CE [9] considering the CSI feedback. In CSI feedback stage in the conventional CE, each estimate is assumed to be quantized to N_q=8 bits and hence, the CSI feedback of JN_qN_c bits is required. In this paper, it is assumed that the same data modulation as the data stage is used in feedback stage. Therefore, the CSI feedback of $N_qJ/\log_2 M$ blocks is required. Based on above assumptions, the throughput S (bps/Hz) is given as

$$S = \frac{1}{2}(\log_2 M)(1-PER)\left(\frac{N_c}{N_c+N_g}\right)\left(\frac{N_B}{1+N_B+\left(N_qJ/\log_2 M\right)}\right), \quad (33)$$

where M is the modulation level and PER denotes the packet error rate. In this paper, we assume that one packet consists of 2048 bits. By contrast, CSPACE with AWWC does not require the CSI feedback, and hence, the throughput when using CSPACE with AWWC is given by setting N_q=0 in (33).

Fig. 6 plots the throughput performance when using CSPACE with AWWC and the conventional CE [9] as a function of the total transmit power to noise power ratio P_T/N. The performances with the perfect CSI case are also plotted in Fig. 6. It is seen from Fig. 6 that the maximum throughput decreases as the number of RS antennas increases when using the conventional CE. This is because the amount of CSI feedback increases as the number of RS antennas increases. By contrast, CSPACE with AWWC does not require the CSI feedback, and hence, it always provides the throughput performance superior to when using the conventional CE. When the number of RS antennas is J=4, CSPACE with AWWC can achieve about twice higher throughput than the conventional CE.

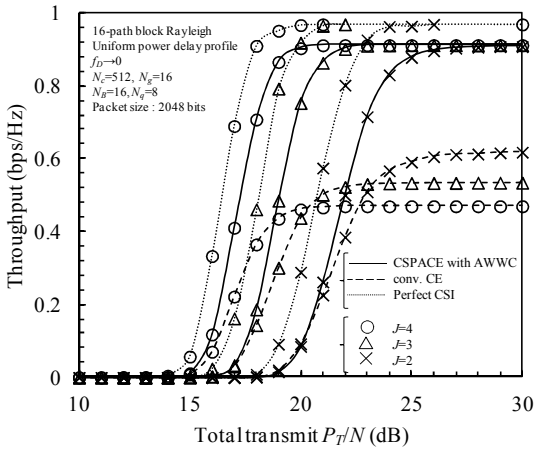

Fig. 6 Throughput performance.

TABLE I. COMPUTATIONAL COMPLEXITY FOR CSPACE WITH AWWC

AWWC		FDCE	
Delay time-domain windowing and noise power estimation	$2N_c$	FFT	$5N_c \log_2 N_c$
Approximated function estimation	$<7N_c$	Reverse modulation	$2N_c$
Window width update	4	IFFT	$5N_c \log_2 N_c$
Total complexity	$9IN_c+4I$	Total complexity	$10N_c\log_2 N_c+2N_c$

VI. CONCLUSION

In this paper, we proposed an adaptive window width control (AWWC) for CSPACE suitable for SC-ANC-MBDR using joint transmit/receive MMSE-FDE. The proposed AWWC adaptively changes the delay time-domain window width according to the changing channel condition so as to minimize MSE between the channel estimates and the actual channels. It was confirmed by the computer simulations that CSPACE with the proposed AWWC can achieves better BER and throughput performances than CSPACE with fixed window width and the conventional CE. In this paper, the impulse response of equivalent channel was assumed to be approximated as an exponential function. The proof of this approximation is left as our future work. We considered ANC-MBDR with single multi-antenna relay. An extension to multiple multi-antenna relays is also left as our future study.

REFERENCES

[1] J. G. Proakis and M. Salehi, *Digital communications*, 5th ed., McGraw-Hill, 2008.

[2] J. G. Laneman, D. N. C. Tse, and G. W. worwell, "Cooperative diversity in wireless networks: efficient protocol and outage behavior," IEEE Trans. Inf. Theory, Vol. 50, No. 12, Dec. 2004.

[3] S. Katti, S. Gollakota, and D. Katabi, "Embracing wireless interference: analog network coding," Proc.ACMCOMM, pp. 397-408, Aug. 2007.

[4] H. Gacanin, and F. Adachi, "Broadband analog network coding," IEEE Trans. Wireless Commun., Vol. 9, No. 5, pp. 1577-1783, May 2010.

[5] S. Zhang, S. C. Liew, and P. P. Lam, "Hot topic: physical-layer network coding," in Proc ACM 12th MobiCom 2006, pp. 358-365, Sep. 2006.

[6] R. Zhang, C. C. Chai, Y. –C Liang and S. Cui, "On capacity region of two-way multi-antenna relay channel with analogue network coding," IEEE intern. Conf. on Commun., Vol. 27, No. 5, pp. 699-712, Jun. 2009.

[7] R. Zhang, Y. –C Liang, C. C. Chai, and S. Cui, "Optimal beam forming for two-way multi-antenna relay channel with analogue network coding," IEEE J. Sel. Areas Commun., Vol. 27, No. 5, pp. 699-712, Jun. 2009.

[8] H. Miyazaki, N. Nakada, T. Obara and F. Adachi, "Joint transmit/receive MMSE-FDE for MIMO analog network coding in single-carrier bi-directional relay communications," Proc. IEEE 76th Vehiqular Technology Conference, Canada, Sept. 2012.

[9] T. Sjodin, H. Gacanin, and F. Adachi, "Two-slot channel estimation for analog network coding based on OFDM in a frequency-selective fading channel," Proc. 71th IEEE Vehiqular Technology Conference, pp. 1-5, May 2010.

[10] I. Prodan, T. Obara, F. Adachi, and H. Gacanin, "Pilot-assisted channel estimation without feecback for bi-directional broadband ANC," Proc. 17th Asia-Pacific Conference on Communications, Malasia, Oct. 2011.

[11] T. Fujimori, K. Takeda, K. Ozaki, A. Nakajima, and F. Adachi, "Channel estimation using cyclic delay pilot for SC-MIMO multiplexing," IEICE Trans. Commun., Vol. E91-B, No. 9, pp. 2925-2932, Sep. 2008.

[12] S. Haykin, *Adaptive Filter Theory*, Englewood Cliffs, NJ: Prentice-hall, 1991.

[13] D. C. Chu, "Polyphase codes with good periodic correlation properties," IEEE Trans. On Inf. Theory, Vol. 18, Issue 4, pp. 531-532, July 1972.